ASIA-PACIFIC SOLAR RESEARCH CONFERENCE

Peer Reviewed
2017 Solar Research Conference

Azadeh Jafari

The Effect of Turbulence Intensity on the Peak Wind Loads on Heliostats

Azadeh Jafari, Matthew J. Emes, Farzin Ghanadi and Maziar Arjomandi

School of Mechanical Engineering, The University of Adelaide, SA 5005, Australia

E-mail: azadeh.jafari@adelaide.edu.au

Abstract

Highly turbulent wind gusts are critical to the survival of heliostats at stow position. Although it has been indicated that wind loads on heliostats increase with turbulence intensity, the peak loads at very high turbulence interties have not been well studied. This study investigates the effect of turbulence intensities above 20% on peak wind loads on heliostats. Forces on a heliostat model exposed to different levels of turbulence intensity in simulated atmospheric boundary layers have been measured by wind tunnel experiments. In order to generate high turbulence intensities, three sets of spires have been designed and tested in combination with surface roughness elements in the wind tunnel. It was found that the peak lift coefficient is increased by about 77% when the turbulence intensity increases from 7% to 26%. Furthermore, comparison of the normal forces on the mirror panel at stow and operating positions indicated that although the operation normal force coefficient is larger than the stow coefficient, the maximum normal force at stow is significantly larger than the maximum force at operation, especially at higher turbulence intensities.

1. Introduction

Concentrating solar thermal power plants have become increasingly popular for large scale electricity production in the recent years due to the several advantages they possess for large scale electricity production such as the possibility of thermal energy storage and integration with existing fossil fuel power plants (Kolb 2011). A power tower plant consists of a field of heliostat mirrors which reflect sunlight up onto a concentrator at the top of a tower where the concentrated energy is then transferred to a heat transfer fluid. Heliostats are exposed to highly turbulent atmospheric conditions which impose aerodynamic loads on them (Pfahl *et al.* 2017). These loads may lead to structural failure if not accurately accounted for in the design process.

A common practice for reducing loads during wind gusts is reducing the mirror area perpendicular to the wind by aligning heliostats horizontally into a position called the stow position. For a heliostat at stow, the significant force is lift which is caused by the variations in the pressure distribution on the upper and lower surfaces of the plate. While the mean lift and hinge moments are near zero at stow position, the peak forces are about 10-times larger than the mean forces (Peterka *et al.* 1989). In addition, comparison of the wind-induced peak and mean displacements of the heliostat mirror panel at different elevation and wind angles indicates that the ratio of peak to mean displacements is generally higher at stow since the mean loads are lower (Gong *et al.* 2012). This signifies the importance of the consideration of highly turbulent, gusty wind conditions for the survival of heliostats at stow.

The studies in literature have indicated that wind loads are significantly influenced by turbulence intensity (Peterka *et al.* 1989; Pfahl *et al.* 2015; Emes *et al.* 2017). Peterka *et al.* (1989) compared the load coefficients measured at longitudinal turbulence intensities of 14% and 18% with those found for uniform, non-turbulent flow (turbulence intensity = 1.2%). The load coefficients were markedly higher at turbulence intensities above 10%. It is indicated that the peak lift coefficient at stow position increases linearly with longitudinal turbulence intensity at values above 10% (Emes *et al.* 2017). Furthermore, Pfahl *et al.* (2015) found that the peak stow lift and hinge moment coefficients increase by 28% and 53%, respectively, when the longitudinal turbulence intensity rises from 13% to 21%.

However, high turbulence intensities above 20% that correspond to extremely turbulent gusts have not been considered in the previous studies. Underestimation of the wind loads at such conditions can lead to the failure of the heliostat structure and it is therefore of significance to evaluate loads at high turbulence intensities accurately. Hence, this study aims to investigate the effect of turbulence intensity on peak loads, especially at turbulence intensities above 20%.

2. Methodology

Experiments were conducted in a wind tunnel at the University of Adelaide which has a test section with a development length of 17 m and a cross-sectional area of 3 m × 3 m at the wind engineering test section. The wind tunnel is designed for a maximum air speed of 33 m/s and the level of turbulence intensity is between 1% and 3%. A turntable with a diameter of 3 m is positioned 15 m downstream of the vanes. Spires and roughness elements were used to simulate the atmospheric boundary layer. Three sets of spires were designed to achieve different levels of turbulence intensity. The height of the spires was calculated based on the desired power law exponent and boundary layer height using the empirical formula given by Irwin (1981). The first set of spires were designed for a boundary layer height of about 1 m. In order to achieve higher turbulence intensities, the boundary layer height was increased for the next two sets. However, the height of the spires could not be larger than 2 m due to the limited fetch length of the tunnel. Therefore, adopting Kozmar's method for part-depth simulation of the atmospheric boundary layer (Kozmar 2011), the spires were truncated to allow the generation of the lower part of boundary layers of 2.6 m and 4 m thickness by set 2 and set 3, respectively. The spires were followed by a 10 m fetch of wooden roughness elements of 90 mm × 90 mm cross section and 45 mm height. The experimental test setup and the dimensions of the three spire sets are illustrated in Figure 1.

A Turbulent Flow Instrumentation (TFI) Cobra probe with a sampling frequency of 2 kHz was used to measure the three components of velocity. Data were collected at a freestream velocity of 11.5 m/s. The velocity and turbulence intensity profiles are shown in Figure 2(a) and Figure 2(b), respectively. The velocity profiles in the lower 1 m of the boundary layer match with a logarithmic profile with a roughness height of 0.02 m in full scale for spire sets 1 and 2 with a maximum error of 4% and 6%, respectively. The velocity profile of spire set 3 also represents a logarithmic profile with a roughness height of 0.06 m in full scale within a maximum error of 12% at heights between 0.4 m and 0.6 m. As highlighted by the shaded region in Figure 2b, the longitudinal turbulence intensity for the three spire sets is between 6% and 26% at heights between 0.4 m and 0.6 m where the heliostat is stowed.

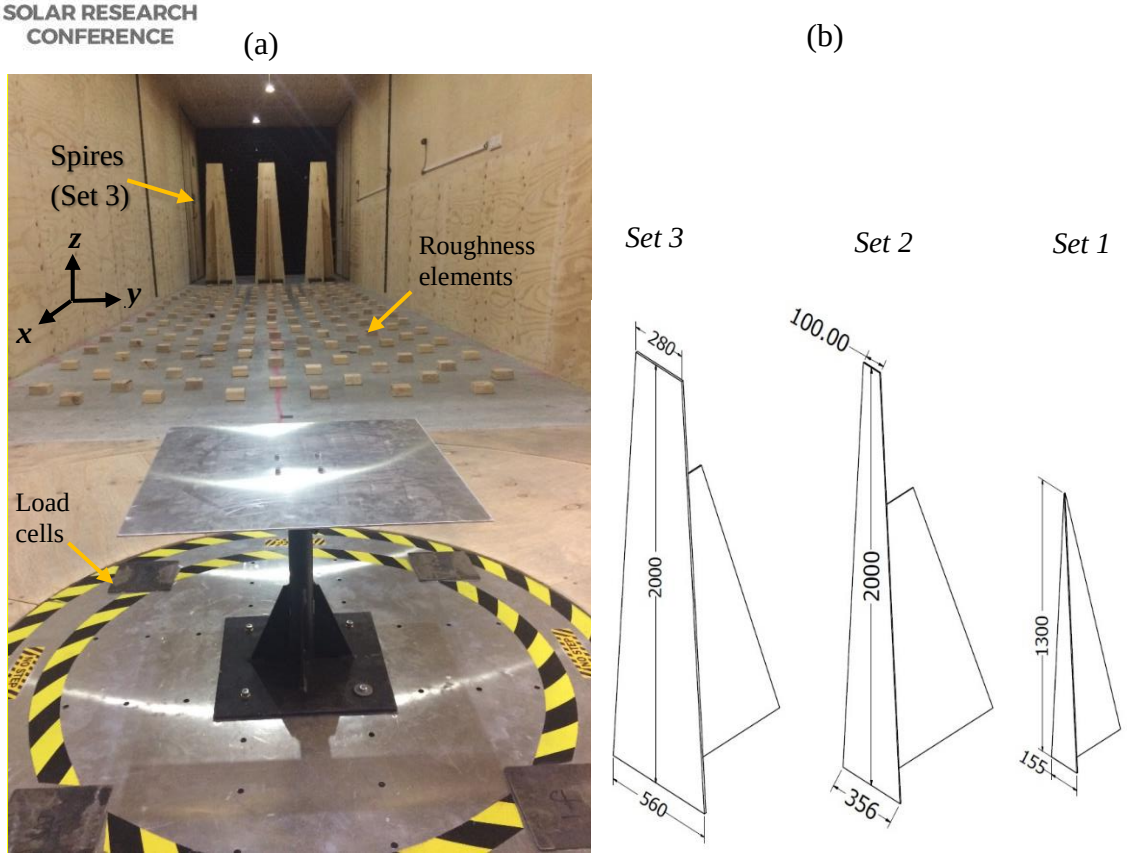

Figure 1 (a) Experimental test setup (b) Dimensions of the three spire sets (in mm)

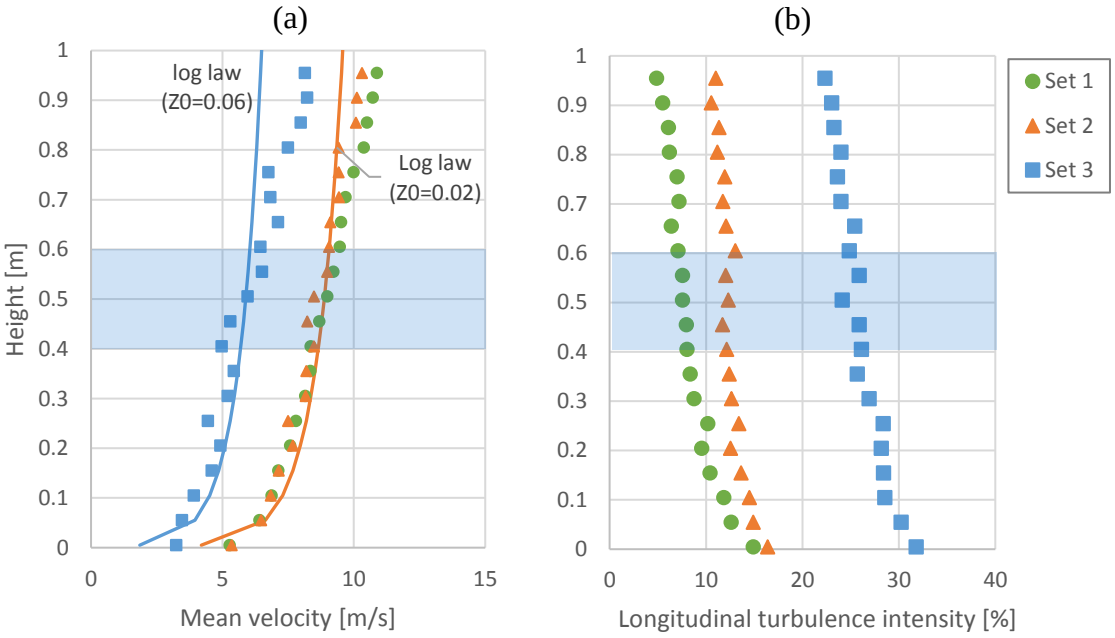

Figure 2 (a) Mean velocity profile (b) Longitudinal turbulence intensity profile

Four three-axis Bestech load cells, each of a capacity of 500 N and a sampling frequency of 1 kHz and an accuracy of ±0.5%, mounted on a rotary turntable were used for measuring forces on the model heliostat. The heliostat models were built by mounting a square aluminium plate of 800 mm × 800 mm and 3 mm thickness on a pylon.

Forces on the heliostat, which are shown in Figure 3, were measured over a sampling period of 60 seconds. The peak values were calculated by the three-sigma approach as the sum of the mean value and three-times the root mean square of the fluctuating forces. The force coefficients are then determined by the following equation:

$$C_i = \frac{F_i}{\frac{1}{2}\rho U^2 A} \quad (i = L, N) \tag{1}$$

where L and N represent lift and the normal force on the mirror panel. U and A show the mean velocity at the heliostat hinge height and the panel area normal to the flow, respectively.

The hinge moment coefficient is calculated by:

$$C_{MHy} = \frac{M_{Hy}}{\frac{1}{2}\rho U^2 A} \tag{2}$$

where $M_{Hy} = L \times p_c$ is the hinge moment and p_c represents the distance to the pressure centre which is assumed to be equal to $0.15 \times c$ (Emes *et al.* 2017).

Figure 3 (a) Main wind loads on a heliostat at stow position (b) Normal force on the stowed mirror panel

3. Results and Discussion

The effect of longitudinal turbulence intensity on peak lift coefficient and hinge moment coefficient at stow position is demonstrated in Figure 4(a) and Figure 4(b). Figure 4(a) shows that the lift coefficient increases by 77% when the turbulence intensity increases from 7% to 26%. The peak coefficients reported by Peterka *et al.* (1989) and Pfahl *et al.* (2015) are also shown for comparison. Peterka's results show an 80% rise in the lift coefficient when the turbulence intensity increases from 14% to 18%. The trend reported by Pfahl *et al.* (2015) is in agreement with the results of the current study. However, the differences in the magnitude of the coefficients found in different studies are related to the different chord lengths of the heliostat models that result in a difference in the relative size of the integral length scales to the

chord length which has been shown to have a significant effect on the peak lift and hinge moment coefficients in stow position (Emes *et al.* 2017).

According to Figure 4(b), a similar trend as the lift coefficient is observed for the hinge moment coefficient. It must be noted that the location of the pressure centre may vary as turbulence intensity increases. Therefore, in order to evaluate the effect of turbulence intensity on hinge moment more accurately, the pressure centre for each turbulence intensity must be determined by evaluation of the pressure distribution on the panel.

(a)

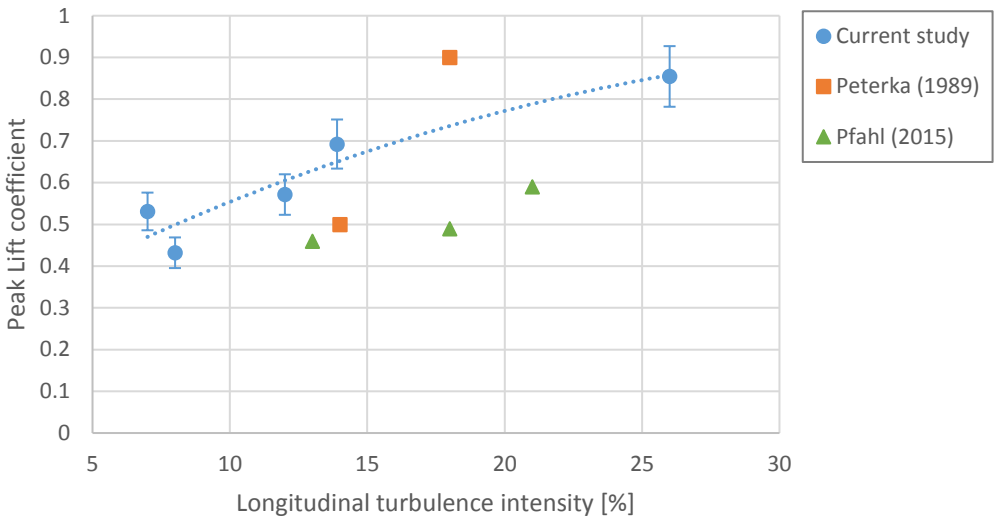

(b)

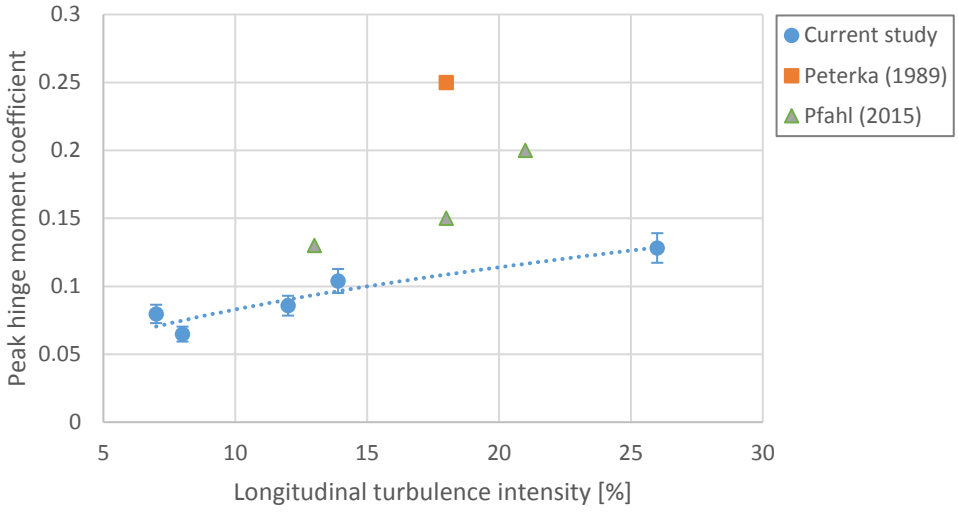

Figure 4 The effect of longitudinal turbulence intensity on (a) peak lift coefficient (b) peak hinge moment coefficient on a stowed heliostat

In order to examine the effect of turbulence intensity on wind loads on heliostats, the force on the heliostat mirror panel is compared at stow and operation positions as a function of turbulence intensity. The peak normal force coefficient at stow and the maximum operation peak normal force coefficient are plotted for different turbulence intensities in Figure 5. The maximum operation normal force coefficient, which corresponds to the normal position, is 3 to 4 times higher than the stow coefficient at longitudinal turbulence intensities between 6% and 26%. However, it is important to note that the wind speeds the heliostat needs to withstand are higher at stow position, which result in larger forces. This can be investigated by the estimation of the peak loads on the CSIRO heliostat with an area of 7.22 m^2 that is designed for a maximum wind speed of 40 m/s at stow and 15 m/s at operation (Coventry *et al.* 2016). Figure 6 shows the normal force on the mirror panel at the maximum operating and stow wind speeds, 15 m/s and 40 m/s, respectively, for turbulence intensities between 6% and 26%. The maximum normal force in stow position is overall larger due to the higher wind speed. Furthermore, the stow load is remarkably larger at high turbulence intensities such that the normal force at stow is 116% larger than the operating force when the turbulence intensity is 26% while at a turbulence intensity of 6%, the stow force is 63% higher. The normal force is also calculated using the coefficients found by Peterka *et al.* (1989) and the results agree in indicating that at a certain turbulence intensity the normal force on the mirror panel is larger at the maximum stow wind speed in comparison to the maximum operating speed.

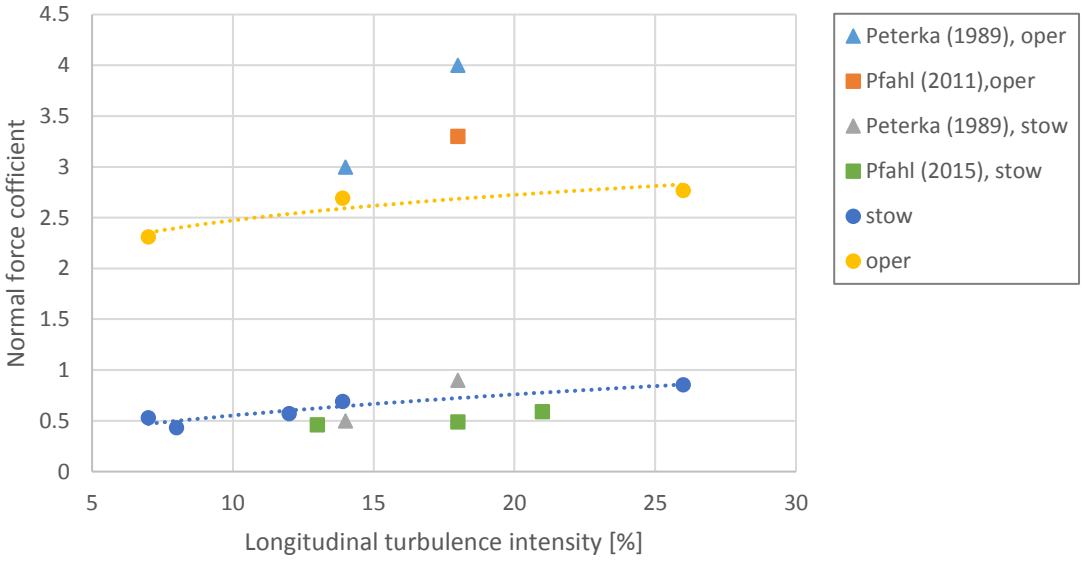

Figure 5 Peak normal force coefficient at stow and operation as a function of turbulence intensity

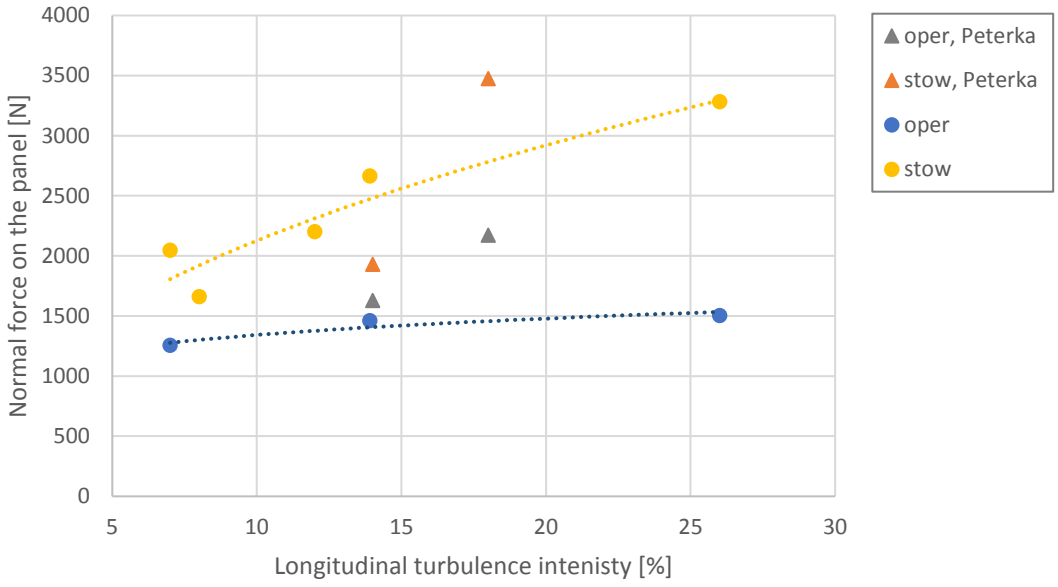

Figure 6 The peak normal force on the mirror panel at maximum operating and stow speeds for a 7.22 m^2 heliostat as a function of turbulence intensity

4. Conclusion

The effect of turbulence intensity on the wind loads on heliostats has been investigated by wind tunnel experiments. It was found that increasing turbulence intensity from 7% to 26% led to a 77% increase in the peak lift coefficient at stow position. Furthermore, comparison of the stow and operating normal force coefficients showed that the operating normal force coefficient is higher than the stow coefficient over a range of turbulence intensities between 6% and 26%. However, the maximum normal force on the mirror panel is significantly larger at stow compared to the maximum operating load due to the higher wind speed, such that the maximum normal force at stow is 116% larger than the operating force at a turbulence intensity of 26%. These results indicate the significance of consideration of the peak forces on stowed heliostats during highly turbulent, gusty wind conditions for the design of heliostats.

References

Coventry, J., Campbell, J., Xue, Y. P., Hall, C., Kim, J. S., Pye, J., Burgess, G., Lewis, D., Nathan, G., Arjomandi, M., Stein, W., Blanco, M., Barry, J., Doolan, M., Lipinski, W., and Beath, A., 2016. 'ASTRI Heliostat cost down scoping study'.

Emes, M. J., Arjomandi, M., Ghanadi, F., and Kelso, R. M., 2017. 'Effect of turbulence characteristics in the atmospheric surface layer on the peak wind loads on heliostats in stow position', *Solar Energy*, 157,p284-97.

Gong, B., Li, Z., Wang, Z., and Wang, Y., 2012. 'Wind-induced dynamic response of Heliostat', *Renewable Energy*, 38,p206-13.

Irwin, H. P. A. H., 1981. 'The design of spires for wind simulation', *Journal of Wind Engineering and Industrial Aerodynamics*, 7,p361-66.

Kolb, G. J., Ho, C.K., Mancini, T.R., and Gary, J.A., 2011. 'Power tower technology roadmap and cost reduction plan', *SAND2011-2419*.

Kozmar, H., 2011. 'Truncated vortex generators for part-depth wind-tunnel simulations of the atmospheric boundary layer flow', *Journal of Wind Engineering and Industrial Aerodynamics*, 99,p130-36.

Peterka, J. A., Tan, Z., Cermak, J. E., and Bienkiewicz, B., 1989. 'Mean and peak wind loads on heliostats', *Journal of solar energy engineering*, 111,p158-64.

Pfahl, A., Coventry, J., Röger, M., Wolfertstetter, F., Vásquez-Arango, J. F., Gross, F., Arjomandi, M., Schwarzbözl, P., Geiger, M., and Liedke, P., 2017. 'Progress in heliostat development', *Solar Energy*, 152,p3-37.

Pfahl, A., Randt, M., Meier, F., Zaschke, M., Geurts, C. P. W., and Buselmeier, M., 2015. 'A holistic approach for low cost heliostat fields', *Energy Procedia*, 69,p178-87.

Acknowledgements

Support for the work has been provided by the Australian Government Research Training Program and the University of Adelaide Scholarship and by the Australian Solar Thermal Research Initiative (ASTRI) through funding provided by the Australian Renewable Energy Agency (ARENA).